Exp Brain Res (2006) 168: 106–119
DOI 10.1007/s00221-005-0074-2

RESEARCH ARTICLE

Jun Xiao · Camillo Padoa-Schioppa · Emilio Bizzi

Neuronal correlates of movement dynamics in the dorsal and ventral premotor area in the monkey

Received: 2 October 2003 / Accepted: 18 May 2005 / Published online: 22 September 2005

Abstract We investigated how neurons in the different motor areas of the frontal lobe reflect the movement dynamics, and how their neuronal activity undergoes plastic changes when monkeys adapt to perturbing forces (they learn new dynamics). Here we describe the results obtained in the dorsal premotor area (PMd) and ventral premotor area (PMv). Monkeys performed visually instructed, delayed reaching movements before, during and after exposure and adaptation to a viscous, curl force field. During movement planning (i.e., during an instructed delay that followed the *cue* and preceded the *go* signal), we found dynamics-related activity in PMd but not in PMv. A closer analysis revealed that the population of PMd reflected the dynamics of the upcoming movement increasingly over the course of the delay, starting from a kinematics-related signal. During movement execution, dynamics-related activity was present in both PMd and PMv. In this respect, the results for PMd were similar to that previously found for the supplementary motor area (SMA) whereas the results for PMv were more similar to that previously found for the primary motor cortex (M1). Plastic changes associated with the acquisition of new dynamics found in PMd and PMv were qualitatively similar to those previously observed in M1 and SMA. The ensemble of our experiments suggest a broader picture of the cortical control of movements, whereby multiple areas all contribute to the various sensorimotor processes, including "low" computations such as the movement dynamics, but also express a degree of specialization.

Keywords Force field adaptation · Internal model · Kinematics-to-dynamics transformation · Motor learning · Monkey

J. Xiao · C. Padoa-Schioppa · E. Bizzi (✉)
McGovern Institute for Brain Research,
Department of Brain and Cognitive Sciences,
Massachusetts Institute of Technology,
Cambridge, MA 02139, USA
E-mail: ebizzi@mit.edu
Tel.: +1-617-2535769
Fax: +1-617-2585342

J. Xiao
Department of Biology, City College of New York,
New York, USA

C. Padoa-Schioppa
Department of Neurobiology, Harvard Medical School,
Boston, MA 02115, USA

Introduction

Execution of visually guided reaching movements involves a sequence of computational stages, including processing of movement kinematics and dynamics. With respect to the neurophysiological processing of movement dynamics, past work largely focused on the primary motor cortex (M1). Numerous experiments confirmed the original observation of Evarts (1968) that the activity of neurons in M1 reflects the presence of external loads (Thach 1978; Fromm 1983; Kalaska et al. 1989; Crutcher and Alexander 1990; Li et al. 2001). The main focus on M1 is possibly due in part to a "serial" view of the motor system, according to which "premotor" areas harbor early sensorimotor processes and funnel their output into M1, which directly controls the execution of movements. The serial view suggests that the processing of the dynamics —a "late" computational stage —might be largely confined to M1. Anatomical evidence, however, has shown that direct corticospinal projections originate from multiple areas, including the supplementary motor area (SMA), the dorsal premotor area (PMd), the ventral premotor area (PMv), the cingulate motor areas (CMAs), in addition to M1 (He et al. 1993, 1995; Rouiller et al. 1996). It was also shown that these areas are heavily interconnected with each other (Luppino et al. 1993, 1994).

One potential consequence of these remarkable findings is that all these areas may possibly participate in late motor processing stages —and in particular the

movement dynamics. With respect to SMA, this hypothesis was demonstrated true by the studies of (Alexander and Crutcher 1990) and more recently by our experiments (Padoa-Schioppa et al. 2002, 2004). Both sets of studies found that the activity on neurons in SMA varies depending on the presence of external loads or forces. Force-dependent activity is observed during motor execution, similarly to what is found in M1, but also during motor planning, when most cells in M1 lack directional tuning. Most interestingly, we found that the activity of neurons in SMA reflects the movement dynamics increasingly during motor planning, starting from a kinematics-related signal (Padoa-Schioppa et al. 2002).

In the present article, we extended our survey of the dynamics-related activity of cortical motor areas to PMd and PMv. With respect to PMd, previous work mostly searched to differentiate this area from M1 for its involvement in "high" sensorimotor processes. It was found that neurons in this area activate before expected visual signals (Mauritz and Wise 1986) and during motor preparation (Wise and Mauritz 1985; Kurata and Wise 1988). In addition, target-related activity prior to and during movement was found more frequently in PMd than in M1 (Shen and Alexander 1997a, b). This notwithstanding, many authors reported extensive functional overlaps between PMd and M1 (Riehle and Requin 1989; Crammond and Kalaska 1994, 1996; Johnson et al. 1996, 1999; Scott and Kalaska 1997; Scott et al. 1997). Regarding the hypothesis of dynamics-related activity in PMd, the most relevant study by Werner et al. found that the activity of 26% of PMd cells co-varied monotonically with a static torque in an isometric task (Werner et al. 1991). This result indeed suggested that neurons in this area might participate in the processing of the movement dynamics.

The properties of area PMv have become under interest relatively recently, and are still largely unclear. Graziano et al. found that neurons in this area respond to both visual and tactile stimulation, and to proprioceptive inputs (Graziano et al. 1997; Graziano 1999). Reports on PMv seem to defy the notion that "early" activity corresponds to "high" computations. On the one hand, neurons in PMv reflect processes in extrinsic coordinates more often than neurons in M1 do (Kakei et al. 2001), and effector-independent activity is more frequent in PMv than in PMd (Hoshi and Tanji 2002). On the other hand, neurons in PMv present premovement activity less frequently than neuron in PMd do (Boudreau et al. 2001). One possibility is, of course, that the area needs further subdivision and that recording sites varied in different experiments. For example, the anatomy work of He et al. (1993) showed that corticospinal projections from PMv were dense, but confined to a small sub-region. Most relevantly for the current discussion, Hepp-Reymond and colleagues found in PMv two clusters of neurons whose activity co-varied with an external force in precision grip task (Hepp-Reymond et al. 1994, 1999), a result consistent with the hypothesis that PMv might participate to processing of the movement dynamics.

Materials and methods

The experimental setup, recording techniques and data analysis were essentially the same previously described (Li et al. 2001; Padoa-Schioppa et al. 2002), with minor differences. The NIH Guide for the Care and Use of Laboratory Animals was followed throughout the experiments.

Behavioral paradigm

Two young female rhesus monkeys (R and N), weighting 5–5.5 kg, participated in the experiment. The monkeys sat on a chair in an electrically isolated enclosure. With their right arm, they held the handle of a two degrees of freedom robotic arm (the manipulandum), which allowed free movements limited to a horizontal plane. A computer monitor, placed vertically 75 cm in front of the monkeys, indicated the position of the handle (3 mm×3 mm square, 0.2° of visual angle) and the targets of the movements (12×12-mm squares, 1° of visual angle). All reaching movements were from a central location to one of eight peripheral targets, equally spaced along a circle and 45° apart from each other. Actual reaching movements were 6 cm in length.

Monkeys performed an instructed delayed reaching task. At the beginning of each trial, monkeys moved the cursor inside a square placed in the center of the monitor. After 1 s, one peripheral target appeared in one of the eight possible locations (*cue*). Monkeys maintained the cursor in the center location for a randomly variable delay (1.1–1.9 s), at the end of which the center square was extinguished (*go*). Monkeys had to acquire the peripheral target within 1.8 s and to maintain the cursor within the peripheral target for 1 s to receive a juice reward (*rew*). After an inter-trial interval (*iti*) of 1 s, the sequence started over again. During the movement, the monkeys had to maintain the trajectory within an angle of 60° on each side of the straight line passing through the center and the peripheral target. The trial was immediately aborted if the monkey made an error. Peripheral targets were pseudo-randomly chosen.

Two motors attached at the base of the robotic arm allowed turning force fields on and off. In the experiment, we used one of two force fields, described by $\mathbf{F} = \mathbf{BV}$, where $\mathbf{B}$ is an anti-diagonal 2×2 rotation matrix $\mathbf{B} = [0, -b; b, 0]$ and $\mathbf{V}$ is the instantaneous velocity vector. Thus, the forces were in strength proportional to the velocity (viscous) and in direction orthogonal to the velocity (curl). Depending on the sign of "b", this defined one of two force fields, clockwise (CK) or counterclockwise (CCK). For the intensity of the forces, we used $b = 0.07$ N/cm. In each experimental session, the monkeys performed in three subsequent behavioral

conditions: Baseline (no force, ca. 160 trials), Force (ca. 160 trials), Washout (no force, ca. 160 trials). In the Force condition, one of the two force fields (CK or CCK) was introduced. The same timing and spatial constraints were maintained throughout the session.

Previous work shows that upon adaptation to curl force fields, the electromyographic (EMG) activity of muscles activated during the movement undergoes systematic changes. Specifically, muscles tuning curves rotate in the direction of the external force. Their preferred direction shifts on average by 18–22° (Li et al. 2001), a result analogous to that found for humans (Thoroughman and Shadmehr 1999; Shadmehr and Moussavi 2000). A similarly consistent rotation observed in the tuning curve of cortical neuron can be regarded as a fingerprint of dynamics-related activity.

During the training (4–6 months), the monkeys performed in nonperturbed conditions. The force fields were introduced only during the recordings. In total, monkey R performed in 28 and 27 sessions with the CK and CCK force fields, respectively. Monkey N performed four and five sessions with the CK and CCK force fields, respectively. For both monkeys, sessions with the two force fields were interspersed.

Surgery, microstimulation and gross anatomy

Before the training and under aseptic stereotaxic surgery, we implanted a head-restraining device on the skull of the monkeys. At the end of training, we implanted a recording chamber (18 mm, inner diameter) over the left hemisphere. For both monkeys, we centered the chamber on ($A = 16$, $L = -15$). After surgeries, the monkeys were given antibiotics (Baytril 2.5 mg/kg IM for 7–10 days) and pain medications (Buphrenex 0.01–0.03 mg/kg IM every 6–8 h).

In the days prior to the first recording session and at the end of several recording sessions, we performed electrical microstimulation. We used a train of 20 biphasic charge balanced pulse pairs (0.1 ms pulse width, 60 ms train), delivered at 330 Hz and variable amplitude (20–120 μA). Recordings were concentrated in areas were arm movements could be elicited, although individual cells were not selected for their responses prior to recordings.

Both monkeys were euthanized at the end of the experiment. They were given an overdose of pentobarbital sodium and then perfused transcardially with heparinized saline, followed by buffered Formalin. The recording locations were marked with electrodes dipped in black ink. The brain was then removed from the skull, and photographed.

Recordings

The recording procedures were described previously (Li et al. 2001). Hand trajectories were recorded at the frequency of 100 Hz. For the neuronal recordings, we manually advanced vinyl-coated tungsten electrodes (1–3 MΩ impedance) with a set-screw system. Electrical signals were acquired, passed through a head stage (AI 401, Axon Instruments), amplified (Cyberamp 380, Axon Instruments), filtered (10 kHz and 300 Hz cutoffs), and displayed on a computer monitor (sampling frequency of 20 kHz) using a commercial software (Experimenter's WorkBench 5.3, DataWave Technology). Action potentials —detected by threshold crossing —were saved to disk (waveforms of 1.75 ms duration) for subsequent clustering analysis. Up to eight electrodes, simultaneously, were used in each recording session. No effort was made to locate the cortical layer of the recordings.

Data analysis: psychophysics

For each movement, we defined the movement onset (*mo*) and the movement end (*me*) with a threshold-crossing criterion (4 cm/s) on the speed. The psychophysics was analyzed using a correlation coefficient, as previously described (Shadmehr and Mussa-Ivaldi 1994; Li et al. 2001). In each session, we derived an ideal speed profile $\mathbf{u}(t)$, separately for each movement direction. We subsequently aligned, for each trial, the actual speed profile $\mathbf{s}(t)$ with the ideal speed profile $\mathbf{u}(t)$ at their peaks. The correlation coefficient (CC) was defined as $CC(\mathbf{s},\mathbf{u}) = Cov(\mathbf{s},\mathbf{u}) / (\sigma(\mathbf{s})\ \sigma(\mathbf{u}))$. Thus, CC was a measure of similarity between $\mathbf{s}(t)$ and $\mathbf{u}(t)$. The values of CC ranged between –1 and +1, and were close to +1 for actual speed profiles close to ideal.

In order to compare the neuronal activity across trials with similar kinematics, we disregarded the first four successful trials in each movement direction. Only the remaining trials were considered for further analysis. This criterion was chosen for consistency with previous studies and because it roughly corresponded to the initial adaptation phase.

One of the aims of the experiment was to investigate the neuronal activity related to the movement dynamics during the instructed delay. No time constraints on the reaction time (RT) were imposed during the experiment. In the analysis of the delay activity we excluded anticipated movements ($RT < 200$ ms) as well as outliers ($RT > 500$ ms). Only the remaining trials ($> 89\%$) were considered for subsequent analysis.

Data analysis: neurons

The clustering of waveforms was performed either using a custom-written software as previously described (Li et al. 2001), or with a semi-manual procedure using a commercially available software (Autocut 3, DataWave Technology). In both cases, waveforms were visually inspected for stability. Only and all the cells with convincingly consistent waveform throughout the session were considered for further analysis.

We considered the neuronal activity of single neurons in four separate time windows: the center hold time (CH, 500 ms preceding the *cue*); the delay time (DT, 500 ms preceding the *go*); the movement time (MT, from 200 ms before *mo* to *me*); the target hold time (TH, 500 ms preceding the *rew*). For each neuron and for each time window, the activity was separately analyzed in the Baseline, Force and Washout conditions. For each condition, we averaged the activity across trials, and obtained a tuning curve. Only tuning curves with an average firing rate >1 Hz were considered for further analysis. The preferred direction (Pd) was defined as the direction of the vector average of the eight activity vectors. The Pd was only defined for tuning curves displaying a significantly unimodal distribution across directions, as stated by the Rayleigh test ($P<0.01$; (Fisher 1993).

For the statistical analysis of the population, we used standard methods. Collective shifts of Pd were stated with a circular t test (Fisher 1993) using $P<0.05$.

Kinematics-to-dynamics transformation

The population of neurons in PMd presented a significant shift of Pd in the DT time window in the force condition compared to Baseline (see Results) similar to that previously observed in SMA. We analyzed the time course of this shift for individual neurons and for the population of PMd with the same methods used previously (Padoa-Schioppa et al. 2002). Briefly, we aligned trials in the Baseline and Force conditions at the *cue* and we considered the activity of each cells in 300 ms-wide time bins, centered every 25 ms in the interval ranging from 300 to 1,350 ms after the *cue*. In each time bin, we defined the tuning curve and computed the Pd. We only considered the activity recorded before the *go* signal, so that "late" time bins included fewer trials (the latest time bin centered 1,350 ms after the *cue* included exactly one half of the trials). For each cell, we aligned the Pd so that "zero" was the Pd recorded in the Baseline in the latest time bin considered. For each time bin, we then computed the population Pd shift. The Pd was only defined for those time bins in which the activity of the cell was directionally tuned (Rayleigh test, $P<0.01$). Finally, we operated a linear regression of the population shift of Pd on time. As previously done for SMA, we restricted this regression analysis to the cells whose Pd shift measured at the end of the DT time window was above average.

For the analysis of the "adaptation effect," we quantified the goodness of adaptation with the initial angular deviation of the hand trajectory from the straight path, as previously described (Padoa-Schioppa et al. 2002). We divided trials in two groups depending on the angular deviation (d): well-adapted trials ($d \leq$ median(d)) and poorly-adapted trials ($d \geq$ median(d)). We analyzed the neuronal activity in the DT time window. For the force condition, we computed two separate tuning curves for the two groups of well-adapted trials and poorly-adapted trials. We then computed the Pd and relative shift of Pd (i.e., shift from the Baseline Pd) separately for the two groups of trials. Finally, we compared the shifts of well-adapted and poorly-adapted trials in a population scatter plot.

We used a similar approach for the analysis of the "reaction time (RT) effect." In this case, trials were divided according to the RT into two groups of shortRT and longRT. Separate tuning curves, Pd and Pd-shifts were computed for the two groups of trials and compared in a population scatter plot. Analysis of the RT effect was limited to neurons whose Pd shift measured at the end of the delay was above average.

In all respects these analyses were identical to that previously performed on neurons recorded in SMA.

Classification of cells

Significant changes across conditions were stated using the error-propagation procedure previously described and used (Li et al. 2001). For this analysis, we used the same significance threshold of $P<0.01$ used in a recent study on SMA (Padoa-Schioppa et al. 2004), which is higher than the $P<0.05$ used in the original study of M1 (Li et al. 2001). Cells were divided in classes depending on the changes across behavioral conditions. We named "kinematic" cells that maintained their Pd unchanged across conditions (x–x–x). Cells for which the Pd changed in the Force condition compared to Baseline and returned to the original orientation in the Washout (x–y–x) were named "dynamic" cells, because the dynamics of the movement were the same in the Baseline and the Washout, but different in the Force condition. Cells for which the Pd changed in the Force condition and remained in the Washout in their newly acquired orientation (x–y–y) were named "memory I," because they appeared to keep trace of the adaptation experience after the monkey had re-adapted to the non-perturbed conditions. A complementary group of cells, for which the Pd did not change in the Force condition but changed in the Washout (x–x–y) were named "memory II" cells. Finally, cells for which the Pd changed in the Force condition and again in the Washout (x–y–z) were named "other" cells.

Results

Psychophysics

The present study confirms the psychophysical results previously described for monkeys (Gandolfo et al. 2000; Li et al. 2001; Padoa-Schioppa et al. 2002) and humans (Shadmehr and Mussa-Ivaldi 1994). Analysis of the correlation coefficient provides evidence of motor adaptation across trials within one session (Fig. 1a). Long-term motor learning took place across sessions throughout the recording period (Fig. 1b).

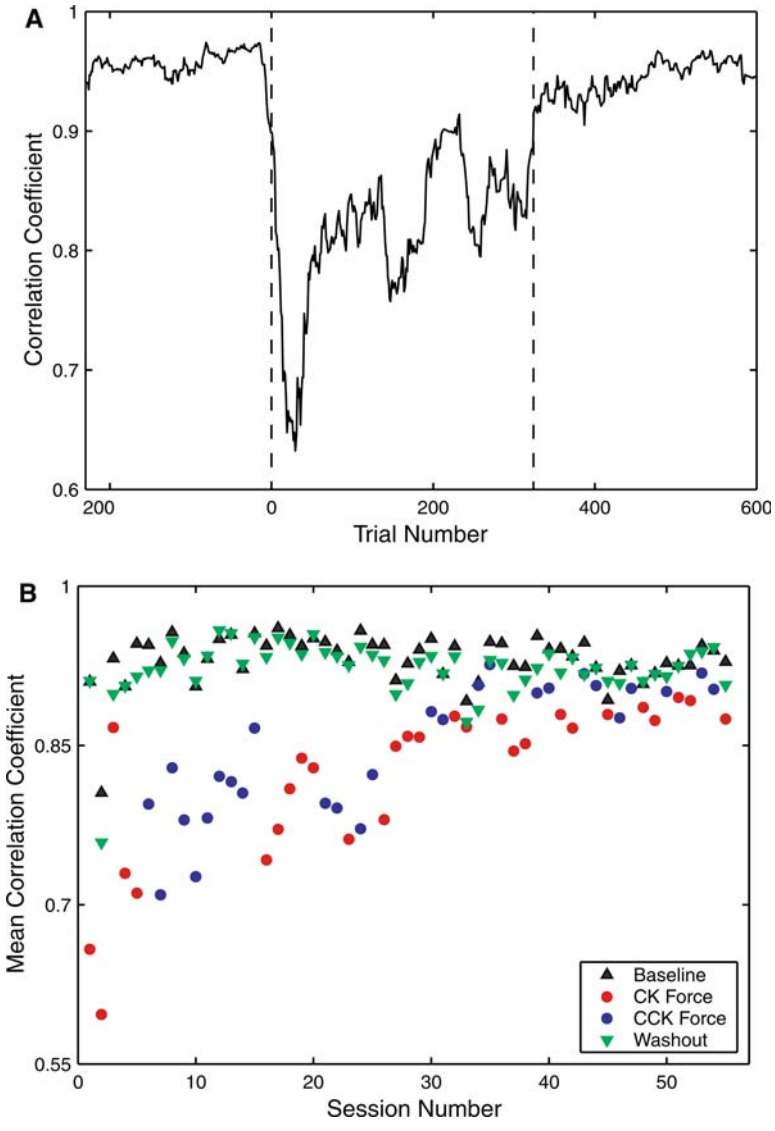

Fig. 1 Psychophysics of the task. **a** Correlation coefficient (CC, *y*-axis) as a function of trial number (*x*-axis) for one representative session. Values of the CC range between –1 and 1, and are close to 1 for movements close to ideal. The CC has high values in the Baseline. It drops at the beginning of the Force condition and gradually recovers as the monkeys adapt to the perturbing force. In the Washout, after a short re-adaptation phase, the CC returns to the high values observed in the Baseline. **b** Over sessions, the adaptation became faster (shorter ramp) and better (higher plateau). This process of long-term learning is illustrated by plotting the mean CC (*y*-axis) against the session number (*x*-axis), separately for the three conditions. Sessions with the CK force field (*red color*) and the CCK force field (*blue color*) were intermixed. For both force fields, the mean CC recorded in the Force condition increased over sessions (long-term learning)

Neuronal database and directional tuning

Following Matelli et al. (1985, 1991), we set the boundaries between PMd and PMv at the spur corresponding to the genu of the arcuate sulcus. We performed microstimulation to identify the arm regions within PMd and PMv. The PMv recordings were carried out on the external surface and in the posterior bank of the arcuate sulcus (Fig. 2). In total, we recorded the activity of 142 PMd cells (108 in monkey R, 34 in monkey N) and 143 PMv cells (133 in monkey R, 10 in monkey N).

The percentages of directionally tuned cells for PMd are shown in Table 1. Considering the Baseline, in the DT 39% of cells in PMd were directionally tuned. The number of directionally tuned cells increased only slightly in the MT, to 46% of cells. In contrast, fewer cells were tuned in the TH (22%). Table 1 shows the corresponding percentages for PMv. For both areas the highest percentage of directionally tuned cells was observed in the MT. The most important difference between the two areas was that in the DT there were many more directionally tuned cells in PMd than in PMv. In the DT time window, we could classify 34/142 = 24% of PMd cells and 9/143 = 6% of PMv cells. Comparing these numbers with a Pearson's χ^2 comparison ([PMd, PMv] × [DT#cells, total#cells]), we obtained a very significant difference ($\chi^2 = 12.9$; df. = 1; $P < 10^{-3}$). Thus, directional tuning occurs in PMd at an earlier time than in PMv. Considering the percentages of directionally tuned cells in the Force and in the Washout conditions (second and third columns in Table 1) strengthened these observations. In the MT time window, we could classify 37/142 = 26% of PMd cells and 26/143 = 18% of PMv cells. PMd and PMv did not differ by this measure ($\chi^2 = 1.6$; df = 1; $P < 0.2$).

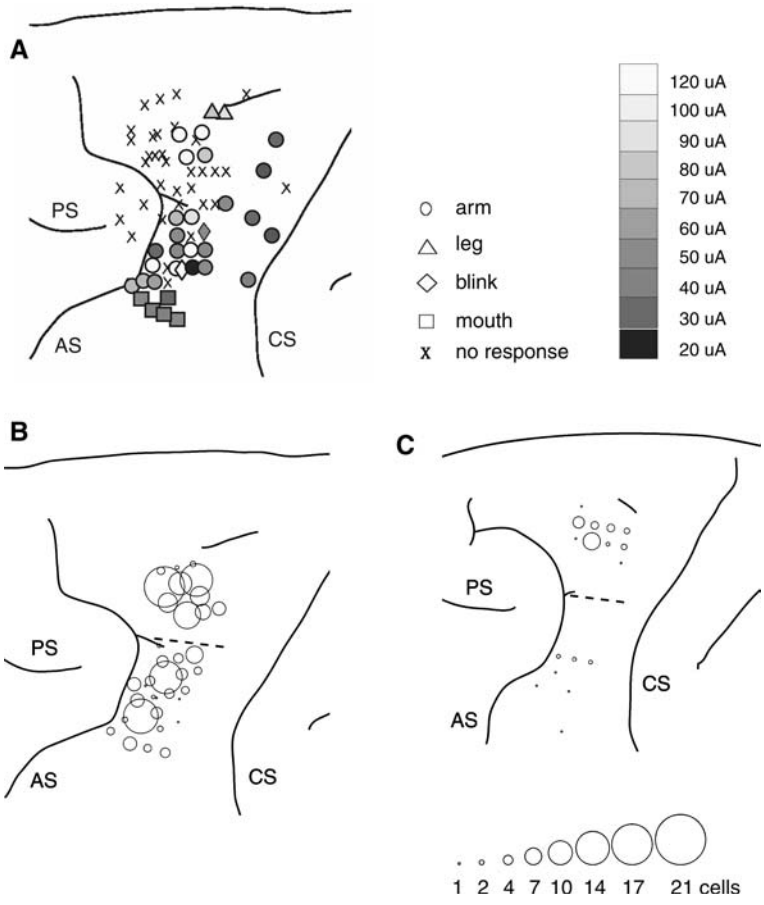

Fig. 2 Microstimulation and recordings. **a** Results of microstimulation for monkey R. *CS* central sulcus, *AS* arcuate sulcus, *PS* principal sulcus. Arm movements could be evoked from both the PMd and the PMv. **b** Reconstruction of the recording sites for monkey R. The radius of the circle indicates the number of cells recorded in the corresponding location, according to the legend. Following Matelli et al (1985, 1991), we located the boundary between PMd and PMv at the spur of the arcuate sulcus (*dotted line*). **c** Recording locations for monkey N

We also analyzed the circular distributions of preferred direction (Pd), separately for the three time windows (DT, MT and TH) and for the three conditions (Baseline, Force and Washout). Circular statistics indicated that the distribution was homogeneous in all three time windows, and in all three behavioral conditions (minimal $P > 0.015$, Rayleigh test). We repeated the same analysis for PMv. Again, we found that the distribution of Pd were homogeneous in all three time windows and all three conditions (minimal $P > 0.035$, Rayleigh test).

Table 1 Number (percentage) of cells directionally tuned

	Baseline	Force	Washout
Dorsal premotor area (PMd)			
CH	4 (3)	2 (1)	2 (1)
DT	56 (39)	61 (43)	47 (33)
MT	65 (46)	72 (51)	68 (48)
TH	31 (22)	35 (25)	24 (17)
Ventral premotor area (PMv)			
CH	6 (4)	12 (8)	2 (1)
DT	35 (24)	30 (21)	27 (19)
MT	69 (48)	61 (43)	56 (39)
TH	22 (15)	29 (20)	27 (19)

In total, we recorded 142 cells from PMd and 143 cells from PMv

Neuronal correlates of movement dynamics in PMd and PMv

With respect to the DT time window, the most interesting results concern PMd. Specifically, we found that the Pd of neurons in PMd shifted significantly in the direction of the external force in the Force condition compared to Baseline. One example of such cells is shown in Fig. 3. This result was consistent at the population level, as illustrated in Fig. 4. On average, the Pd of PMd neurons shifted in the direction of the external force by 10.4° ($P < 0.05$) in the Force compared to the Baseline, and shifted back in the opposite direction in the Washout compared to the Force (mean shift = −8.5°, $P < 0.05$). No net shift of Pd was present in the Washout compared to the Baseline (mean shift = −2.7°, $P = 0.5$). No significant shifts of Pd were observed for the population of PMv in the DT time window.

With respect to MT time window, we found that in both areas cells shifted their Pd significantly in the direction of the external force in the Force compared to Baseline (PMd: mean shift = 11.0°, $P < 0.04$; PMv: mean shift = 11.5°, $P < 0.03$). In the Washout, neurons in both areas shifted their Pd significantly back in the opposite direction (PMd: mean shift = −14.0°, $P < 0.02$; PMv: mean shift = −19.0°, $P < 0.01$). Thus, no net shift of Pd was observed in the Washout compared to the

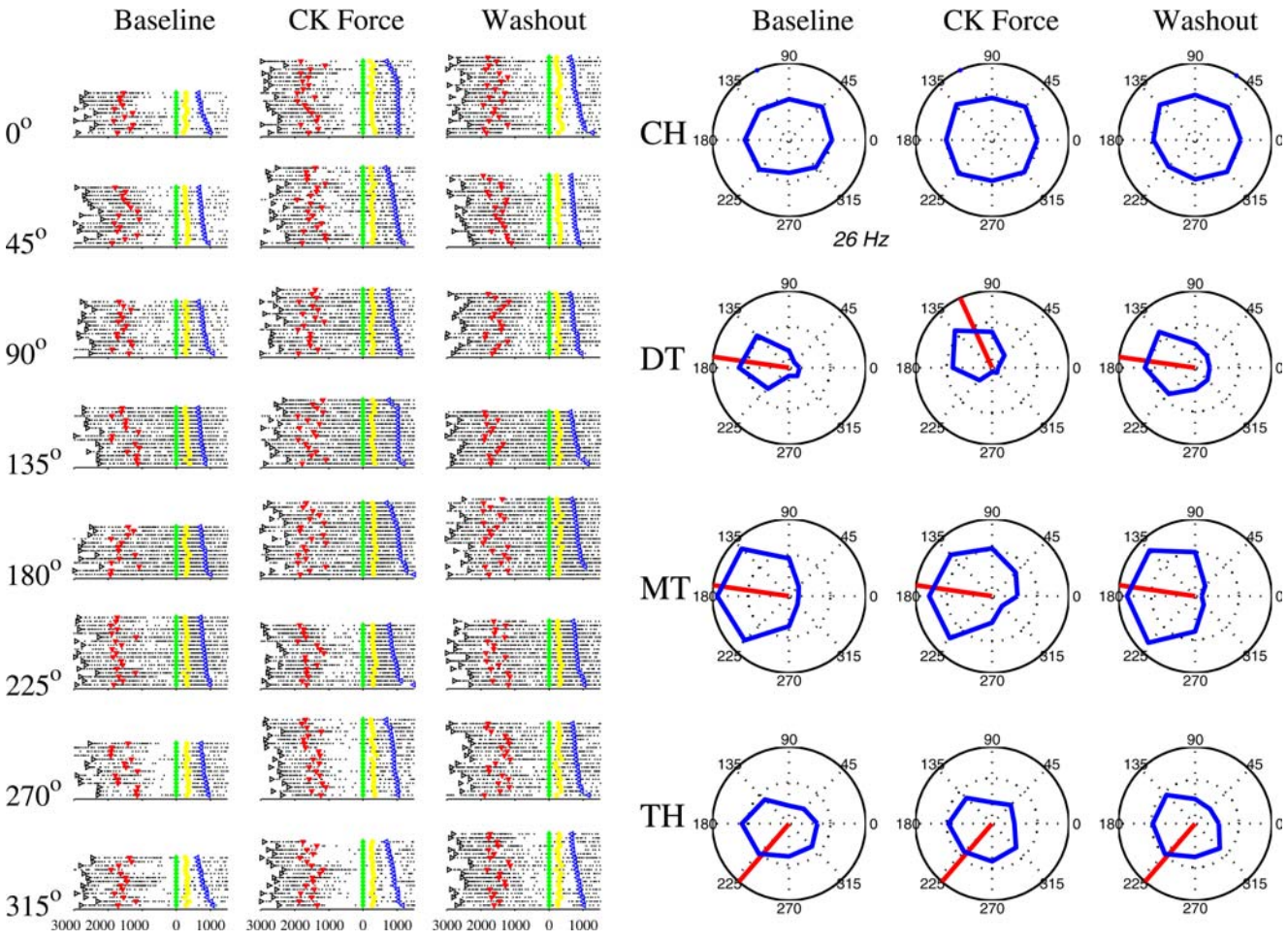

Fig. 3 Rasters and tuning curve of a PMd cell. In the rasters, *color symbols* indicate the beginning of trial (*black*), the presentation of the cue (*red*), the go signal (*green*), the movement onset (*yellow*) and the movement end (*blue*). Here trials are aligned at the go signal and sorted for the movement end time. On the right, the tuning curve for each condition and for each time window is plotted in *blue*. The Pd is plotted in *red*. This cell was recorded with a clockwise force field. It was classified as dynamic for its changes of Pd in the DT time window

Baseline (PMd: mean shift = −6.0°, $P = 0.09$; PMv: mean shift = −11.7°, $P = 0.2$).

No significant shift of Pd was observed in either area in the TH time window.

These shifts of Pd (summarized in Table 2) closely mirror that previously found for neurons in SMA during motor planning, and for neurons in SMA and in M1 and for muscles EMG during movement execution. They indicate that the activity of neurons in PMd reflects the dynamics of the upcoming movement during motor planning. In addition, they indicate that the activity of neurons in both PMd and PMv reflects the movement dynamics during movement execution.

PMd activity and the kinematics-to-dynamics transformation

Figure 5a shows the results obtained for the population of PMd in the Baseline and in the Force conditions. In the Baseline, the population Pd remains essentially constant and close to zero throughout the delay. A linear fit of $\Delta\text{Pd}(t)$ on t failed to indicate significant departures from null slope ($P = 0.08$). In the Force condition, the population Pd is initially aligned with that recorded in the Baseline. Over the course of the delay, however, the Pd of the population progressively shifts in the direction of the external force (positive values on the y-axis). A linear fit of $\Delta\text{Pd}(t)$ on t indicated a slope of 11°/s significantly greater than zero ($P < 10^{-7}$). Thus, neurons in PMd, as a population, appear to reflect the kinematics-to-dynamics transformation.

Figure 5b illustrates the adaptation effect for PMd. In the scatter plot each dot represents one cell. The axes represent the Pd shift for well-adapted trials (x-axis) and the Pd shift for poorly adapted trials (y-axis). We observe that the population tends to lie below the dotted diagonal line bisecting the first and third quadrant. Statistical analysis indicates that this effect is almost significant in PMd ($P < 0.052$). In other words, the shift of Pd recorded in PMd at the end of the delay loosely predicted the initial direction of the upcoming movement.

In SMA, we had found that the shift of Pd recorded in the Force condition in the DT time window anti-

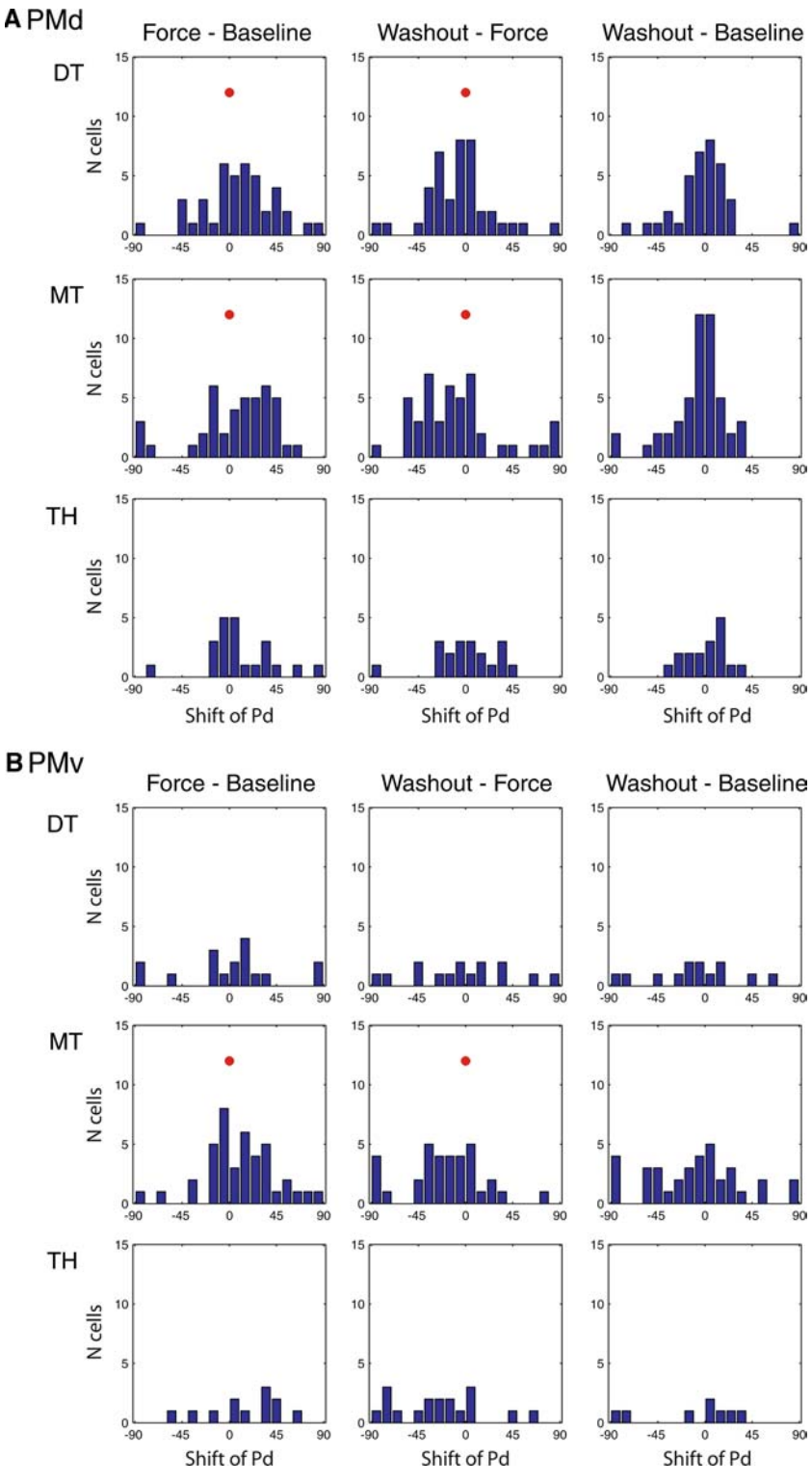

Fig. 4 **a** PMd, population histograms. The histograms illustrate the shift of Pd observed for the entire PMd population in the three time windows DT, MT and TH. Significant shifts of Pd are observed in the DT and MT time windows ($P < 0.05$, circular *t* test, *red dots*). **b** PMv, population histograms. Significant shifts of Pd are observed in the MT time window. Note that some neurons present a negative shift of Pd, a fact for which we lack a satisfactory explanation

correlated with the upcoming reaction time (RT) necessary for the monkey to initiate the movement after the *go* signal. The same analysis on PMd cells failed to reveal a similar significant effect, as illustrated in Fig. 5c. In this case, we computed the shift of Pd in the Force condition (DT time window) separately for shortRT trials (RT $\leq$ median RT) and for longRT trials (RT $\geq$ median RT). In the scatter plot, each dot represents one cell, and the axes represent the Pd shift for shortRT trials (*x*-axis) and the Pd shift for longRT trials (*y*-axis). We would observe a RT effect in PMd if the population of neurons lied significantly below the diagonal dotted line. However, we do not observe such effect in PMd ($P = 0.6$).

Table 2 Population changes of activity (means)

Average Change			
	Force – Baseline	Washout – Force	Washout – Baseline
Dorsal Premotor Area (PMd)			
Change of Pd			
DT	10.4°*	−8.5°*	−2.7°
MT	11.0°*	−14.0°*	−6.0°
TH	10.0°	2.8°	0.8°
Ventral Premotor Area (PMv)			
Change of Pd			
DT	3.1°	0.0°	−6.6°
MT	11.5°*	−19.0°**	−11.7°
TH	15.1°	−27.6°*	−9.2°

*$P < 0.05$, **$P < 0.01$

Consistently, correlates of the kinematics-to-dynamics transformation were rarely observed at the level of individual neurons in PMd. The five panels in Fig. 5d illustrate the time course of the Pd in the delay for five different neurons. For each cell, we superimposed the Pd in the Baseline (black color) to the Pd in the Force condition (red color). Again, "zero" on the *y*-axis is the Pd recorded in the latest time bin in the Baseline. In general, we notice that the Pd is not constant throughout the delay in either the Baseline or the Force condition (Johnson et al. 1999). For the first two cells on the left, we observe that the Pd in the Force condition is very similar to that recorded in the Baseline throughout the delay. For the third and fourth cells, we observe a shift in the Force compared to the Baseline, although that shift did not increase over the course of the delay. In other words, the Pd of these two cells in the Force condition remained rotated at an approximately constant distance throughout the delay from that recorded in the Baseline. Finally, for the rightmost cell, we observe a gradual shift of Pd in the Force compared to Baseline, similar to that observed for individual neurons in SMA. A specific statistical analysis, however, indicated that this was not a consistent finding in PMd. Out of the 20 cells whose Pd shift in the DT time window was greater than average, only three cells presented a significantly increasing Pd shift (linear regression of $\Delta\,\mathrm{Pd}(t)$ on t, $P^* = 0.01$). In contrast, for 12 cells the shift did not increase significantly over the course of the delay. For this analysis, we considered time bins from 300 to 1,300 ms after the *cue*. However, different time limits such as from 300 to 800 ms after the *cue* or from 800 to 1,300 ms after the *cue* provided very similar results. In conclusion, our data do not allow tracing the correlates of the kinematics-to-dynamics transformation down to the activity of individual neurons in PMd.

Field-specific cells, tune-in cells and tune-out cells

As the monkeys adapted to the force field, the directional tuning of cells in PMd and PMv generally changed. For example, some cells were initially not tuned in the Baseline, became tuned in the Force condition, and lost their tuning again in the Washout. Other cells were originally tuned in the Baseline, lost their tuning in the Force condition, but regained their tuning in the Washout. These two groups of cells, which appeared dynamic in nature, were named "field-specific" cells. In total, field-specific cells accounted for 14% of cells in PMd, and for 10% of cells in PMv (MT time window).

We also found two groups of cells whose activity changes outlasted exposure to the force field. "Tune-in" cells were initially not tuned in the Baseline, and acquired a directional tuning in the Force condition following adaptation. In the Washout, however, tune-in cells maintained their newly acquired directional tuning. Similarly, "tune-out" cells were originally tuned in the Baseline, but lost their tuning in the Force condition, and remained nontuned in the Washout. Thus, both tune-in cells and tune-out cells appeared memory in nature. In total, tune-in cells accounted for 16% of PMd cells, and for 15% of PMv cells. Tune-out cells accounted for 14% of PMd cells, and for 25% of PMv cells. Tune-in and tune-out cells were previously described for M1 (Gandolfo et al. 2000).

Motor learning and neuronal plasticity in PMd and PMv

In total, 34 PMd cells could be classified for changes of Pd in the DT time window. Of these, 65% were kinematic, 24% were dynamic, 9% were memory I and 3% were memory II. Figure 6 illustrates the activity of one PMd neuron that was classified as memory I for its changes of Pd in the DT time window.

Of the 143 neurons recorded in PMv, only nine neurons were directionally tuned in the DT consistently in all three conditions (Baseline, Force and Washout) and could therefore be classified according to their changes of Pd. Of these nine neurons, six (67%) neurons were classified as kinematic. The remaining cells were dynamic (one cell) and memory I (two cells).

With respect to the MT time window, a total of 37 PMd cells could be classified according to their changes of Pd. In particular, we found 14 (38%) kinematic cells, 16 (43%) dynamic cells, 2 (5%) memory I cells, 4 (11%) memory II cells, and 1 (3%) "other" cells.

For PMv, we could classify a total of 26 cells according to their changes of Pd in the MT time window. We found that 73% of PMv cells were kinematic, 12% were dynamic, 4% were memory I, 8% were memory II and 4% were "other". Figure 7 illustrates the activity of one PMv cell classified as memory II for its changes of Pd in the MT time window.

Only a limited population of PMd cells (16 cells) could be classified with respect of the changes of Pd in the target hold time (TH). Of these, the vast majority was kinematic (88%).

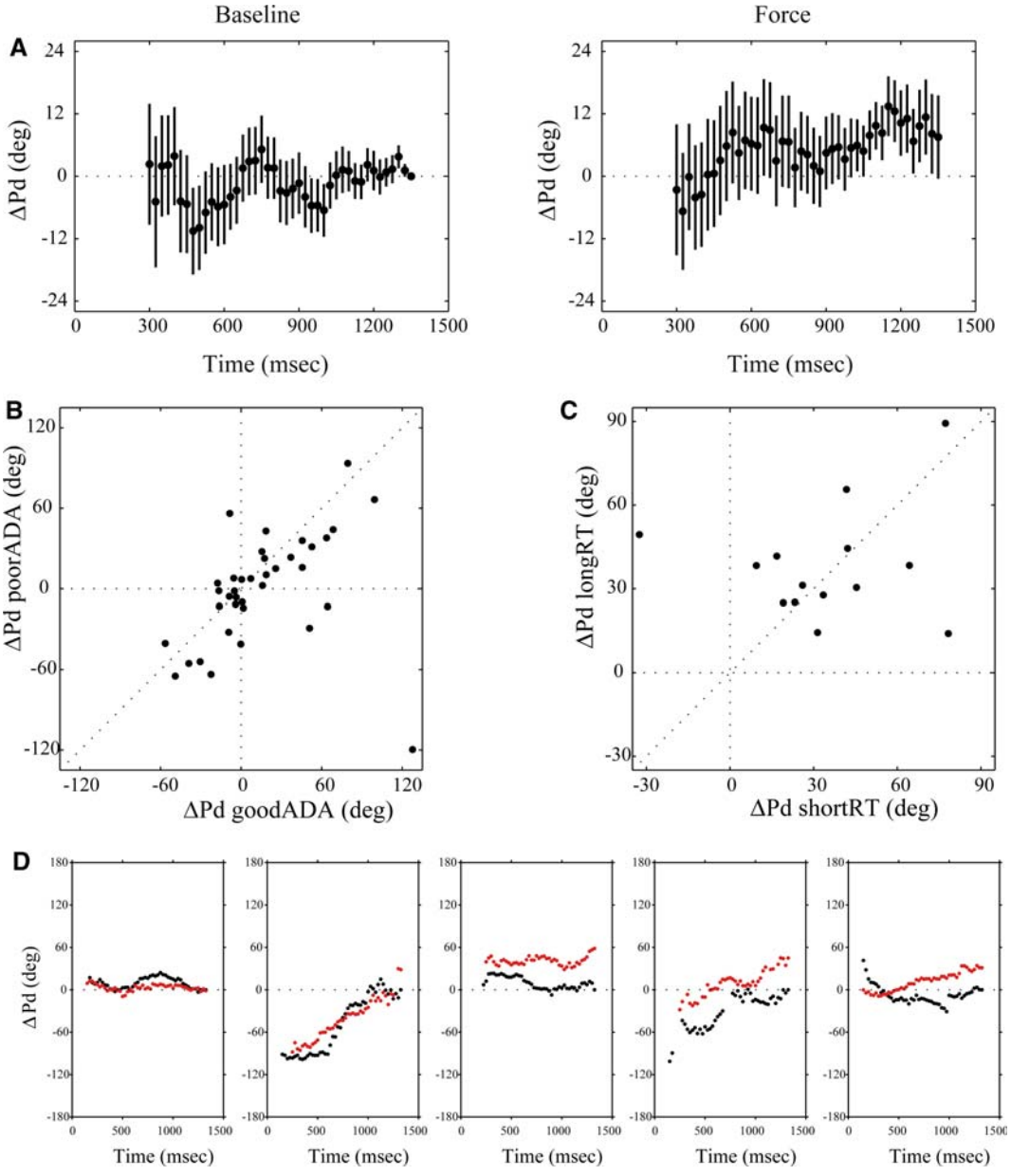

Fig. 5 Neuronal correlates of kinematics-to-dynamics transformation in PMd. **a** Time course of Pd shift during the DT, population. *Solid points* and *vertical bars* indicate the mean and standard deviations and positive values on the *y*-axis indicate shifts of Pd in the direction of the external force. In the Baseline, the population Pd remains roughly constant and close to zero throughout the delay. In the Force condition, the population Pd is aligned with that recorded in Baseline shortly after the *cue* and progressively shifts in the direction of the external force over the course of the delay. Note that we included in this analysis only neuronal activity recorded prior to the *go* signal (see Methods). **b** Shift of Pd and adaptation. *Each dot* in the plot represents one cell. The axes represent the Pd shift for well-adapted trials (*x*-axis) and the Pd shift for poorly adapted trials (*y*-axis). It can be observed that the population tends to lie below the *dotted diagonal line* bisecting the first and third quadrant. **c** Shift of Pd and reaction time. *Each dot* in the plot represents one cell. The axes represent the Pd shift for shortRT trials (*x*-axis) and the Pd shift for longRT trials (*y*-axis). The population of PMd lies similarly above and below the *diagonal dotted line*. Note that this plot contains fewer cells than **b** because in some cases neurons did not pass the tuning criterion for both short-RT and long-RT trials. **d** The five panels illustrate the time course of the Pd for five individual neurons. In each panel, the Pd in the Baseline and Force conditions are superimposed in *black* and *red color*, respectively. Although for all three cells on the right there is a shift of Pd in the Force compared to Baseline at the end of the delay, that shift occurs *progressively* over the course of the delay only for the rightmost cell

A total of eight PMv neurons could be classified according to their changes of Pd in the TH. Of these, seven (88%) neurons were classified as kinematic.

The results of the classification obtained for PMd and PMv in the three time windows are summarized in Table 3.

Considering only the subset of cells with directionally tuned DT activity, we did not find significant differences between PMd and PMv with respect to the proportion of cells in the various classes of kinematic, dynamics, and memory cells ($\chi^2 = 1.1$; df. = 3; $P = 0.8$). The analogous analysis done for the MT time window did show some difference between PMd and PMv ($\chi^2 = 8.2$; df. = 3; $P < 0.05$). In essence, this was because proportionally more cells were classified as kinematic in PMv (19/26 = 73%) than in PMd (14/37 = 38%), whereas more cells were classified as dynamic in PMd (43%) than in PMv (12%). Instead, the proportion on memory cells was similar in the two areas (7/37 = 19% in PMd, 4/26 = 15% in PMv).

Discussion

Neuronal correlates of movement dynamics in PMd and PMv

In this study, we investigated the dynamics-related activity of neurons in PMd and PMv, as revealed by the shift of Pd recorded following adaptation to an external curl force field. With respect to the neuronal activity during the MT, we found that the dynamics of movements is reflected in both PMd and PMv. Significant shifts of Pd were observed both for single cells and for the neuronal populations. Quantitatively, the shifts of Pd recorded during the movement time for the population of PMd (mean shift 11.0° in the Force–Baseline; −14.0° in the Washout–Force) and PMv (mean shift 11.5° in the Force–Baseline; −19.0° in the Washout–Force) are comparable to that recorded in M1 (mean shifts 16.2° in the Force–Baseline; −14.3° in the Washout–Force) and SMA (mean shifts 16.6° in the Force–Baseline; −9.7° in the Washout–Force) (Li et al. 2001; Padoa-Schioppa et al. 2004). This result is consistent with the anatomical fact that direct cortico-spinal projections originate from all these four areas (He et al. 1993, 1995). It is also consistent with previous physiological reports of load-dependent activity in both PMd (Werner et al. 1991) and PMv (Hepp-Reymond et al. 1994, 1999).

PMd and the kinematics-to-dynamics transformation

One important result of the study is that neurons in PMd shift their Pd during the delay time (DT), prior to the *go* signal. This is observed both at the level of single cells and at the level of the population. In other words, during motor planning neurons in PMd reflect the dynamics of the upcoming movement. In this respect, PMd share properties characteristic of SMA (Padoa-Schioppa et al. 2002). In contrast, the activity of cells in PMv is mostly not directionally tuned during the DT, and no significant shifts of Pd are observed in PMv during the DT. In this respect, the activity of neurons in PMv resembles more that previously recorded in M1 (Li et al. 2001; Padoa-Schioppa et al. 2004).

It is generally accepted that execution of visually instructed movements involves a transformation of the desired kinematics into dynamics-related commands (Saltzman 1979; Alexander and Crutcher 1990; Mussa-Ivaldi and Bizzi 2000). In a previous study, we found that neurons in SMA reflect the kinematics-to-dynamics transformation (Padoa-Schioppa et al. 2002). Four lines of evidence implicated neurons in SMA in the kinematics-to-dynamics transformation: the progressive shift of Pd at the level of the population during motor planning; the analogous progressive shift of Pd for individual neurons; the correlation between the Pd shift in the DT time window and the goodness of adaptation (i.e., initial direction of the upcoming movement); and the anticorrelation of the Pd shift in the DT time window and the subsequent reaction time. Two of these phenomena were presently observed also for neurons in PMd, namely the progressive shift of Pd for the population and the adaptation effect. Thus, the neuronal activity of PMd does reflect the kinematics-to-dynamics transformation in a general sense. However, the two phenomena that most directly linked the activation of individual neurons in SMA to the kinematics-to-dynamics transformation, namely the progressive shift of Pd of individual neurons and the reaction time effect, were not systematically found in PMd. Thus, the present results indicate that neurons in SMA do not process the kinematics-to-dynamics transformation in isolation. Neurons in PMd also seem to reflect that transformation, at least as a population, and it is possible that this process involves also other areas (e.g., the basal ganglia, the cerebellum). However, the present results also suggest that neurons in SMA participate more directly to the processing of the kinematics-to-dynamics transformation, whereas neurons in PMd reflect the status of that transformation in a less direct fashion.

Neuronal plasticity in PMd, PMv, M1 and SMA

This series of experiments was designed to investigate the neuronal underpinnings of a specific form of motor learning that takes place when subjects adapt to an external force field. From a psychophysical perspective, this process can be described as the acquisition of a new internal model for the dynamics (Shadmehr and Mussa-Ivaldi 1994; Kawato 1999; Wolpert and Ghahramani 2000). In order to compare the results obtained for different cortical areas, we focused on changes of Pd in the MT time window, and we grouped memory I and memory II cells in a single class of memory cells. In PMd, we recorded 38% kinematic, 43% dynamics, and 16% memory cells. In PMv, we recorded 73% kinematic, 12% dynamics, and 12% memory cells. In contrast, in M1 we recorded 50% kinematic, 17% dynamics, and 32% memory cells. In SMA, we recorded 52% kinematic, 17% dynamics, and 28% memory cells.

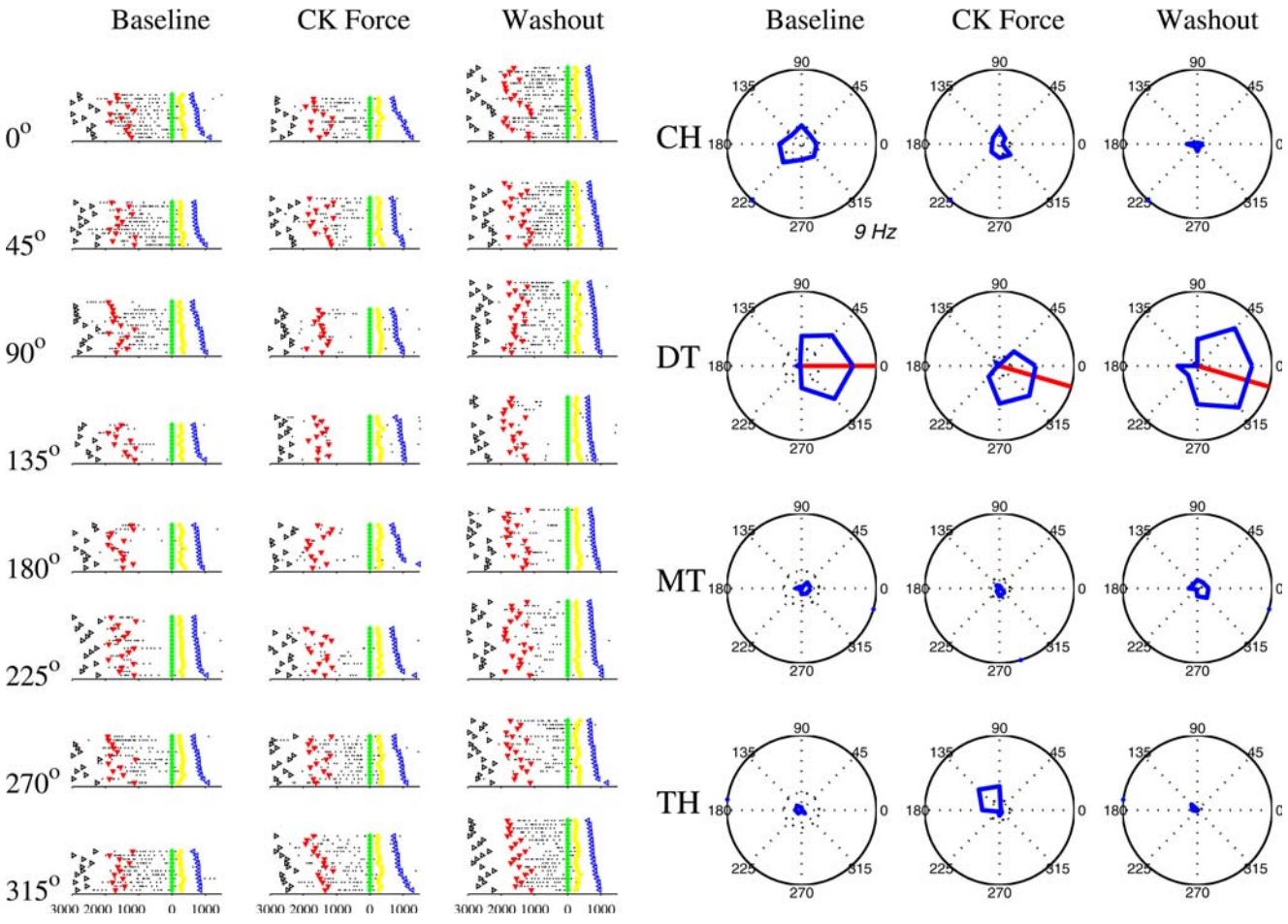

Fig. 6 Rasters and tuning curve of a PMd cell. All the conventions are as in Fig. 3. This cell was recorded with a clockwise force field. It was classified as memory I for its changes of Pd in the DT time window

(Note that the percentage relative to M1 was computed with a significance threshold of $P < 0.01$ more restrictive than $P < 0.05$ used in the original paper (Li et al. 2001).) It can be noticed that in general fewer memory cells were recorded in PMd and PMv compared to M1 and SMA, although a chi-square analysis of these results (two classes of nonmemory and memory cells, four areas) did not indicate a significant difference between areas ($\chi^2 = 4.60$; df = 3; $P = 0.2$). This notwithstanding, the measure of plastic changes generally corroborates the conclusion that dynamics-related signals are stronger in M1 and SMA compared to PMd and PMv.

Conclusion

In conclusion, our experiments indicate that movement dynamics are widely represented across the motor areas of the frontal lobe, including PMd and PMv, SMA and M1. In a broad sense, this result is a physiological counterpart to the anatomical finding that direct corticospinal projections originate from all of these areas, which are also densely interconnected with each other (He et al. 1993, 1995; Luppino et al. 1993).

Our experiments also highlighted important differences between areas. First, as already noticed, there is a sharp distinction between areas PMd and SMA, which participate to motor planning and reflect the kinematics-to-dynamics transformation, and areas M1 and PMv, whose contribution to motor planning appears minimal. Second, we also found a general degradation of the representation of the movement dynamics in PMd and PMv compared to SMA and M1. With respect to motor planning, processing of the kinematics-to-dynamics transformation can be traced down to the activity of individual neurons in SMA, but not individual neurons in PMd. Likewise, the "RT effect" and the "adaptation effect" were present in SMA, but not in PMd. In addition, we generally found less extensive plastic changes associated with learning of an internal model for the dynamics in PMd and PMv than we had found in SMA and M1. In the past few years, two competing views have dominated the debate on the organization of motor system. A serial view states that "premotor" areas harbor "high" sensorimotor processes and funnel their output into M1, which ultimately controls the execution of movements. A parallel view suggests that several motor areas with direct corticospinal projections con-

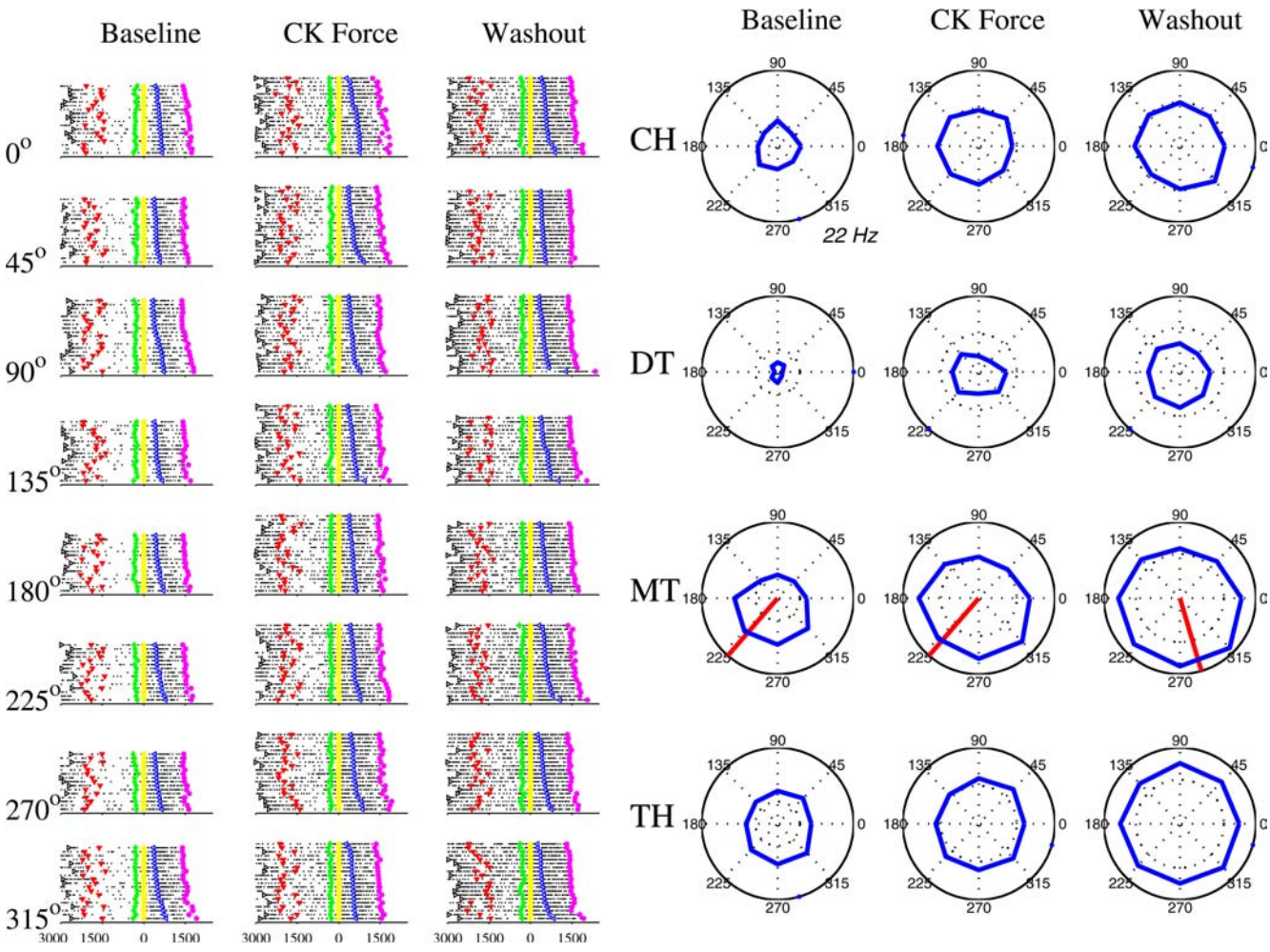

Fig. 7 Rasters and tuning curve of a PMv cell. All the conventions are as in Fig. 3, but in this case we aligned trials at the movement onset. This cell was recorded with a clockwise force field. It was classified as memory II for its changes of Pd in the MT time window

tribute similarly to the preparation and execution of movements. The picture emerging from the series of our studies falls somewhere in between, in that correlates of the movement dynamics, a "low" process, were ubiquitously found in all the areas we recorded from, while clear differences also indicated a degree of area specialization.

Table 3 Number (percentage) of cells in each class

	DT	MT	TH
Dorsal Premotor Area (PMd)			
Kinematic	22 (65)	14 (38)	14 (88)
Dynamic	8 (24)	16 (43)	1 (6)
Memory I	3 (9)	2 (5)	1 (6)
Memory II	1 (3)	4 (11)	0 (0)
Other (*x*-*y*-*z*)	0 (0)	1 (3)	0 (0)
N cells (tot)	34	37	16
Ventral Premotor Area (PMv)			
Kinematic	6 (67)	19 (73)	7 (88)
Dynamic	1 (11)	3 (12)	0 (0)
Memory I	2 (22)	1 (4)	0 (0)
Memory II	0 (0)	2 (8)	1 (13)
Other (*x*-*y*-*z*)	0 (0)	1 (4)	0 (0)
N cells (tot)	9	26	8

Each Table indicates the number (percentage) of neurons in the corresponding class

Acknowledgements This research was supported by the National Institute of Health (NIH grant MN481185).

References

Alexander GE, Crutcher MD (1990) Preparation for movement: neural representations of intended direction in three motor areas of the monkey. J Neurophysiol 64:133–150

Boudreau MJ, Brochier T, Pare M, Smith AM (2001) Activity in ventral and dorsal premotor cortex in response to predictable force-pulse perturbations in a precision grip task. J Neurophysiol 86:1067–1078

Crammond DJ, Kalaska JF (1994) Modulation of preparatory neuronal activity in dorsal premotor cortex due to stimulus-response compatibility. J Neurophysiol 71:1281–1284

Crammond DJ, Kalaska JF (1996) Differential relation of discharge in primary motor cortex and premotor cortex to movements versus actively maintained postures during a reaching task. Exp Brain Res 108:45–61

Crutcher MD, Alexander GE (1990) Movement-related neuronal activity selectively coding either direction or muscle pattern in three motor areas of the monkey. J Neurophysiol 64:151–163
Evarts EV (1968) Relation of pyramidal tract activity to force exerted during voluntary movement. J Neurophysiol 31:14–27
Fisher NI (1993) Statistical analysis of circular data. Cambridge University Press, Cambridge
Fromm C (1983) Changes of steady state activity in motor cortex consistent with the length-tension relation of muscle. Pflugers Arch 398:318–323
Gandolfo F, Li C, Benda BJ, Padoa-Schioppa C, Bizzi E (2000) Cortical correlates of learning in monkeys adapting to a new dynamical environment. Proc Natl Acad Sci USA 97:2259–2263
Graziano MS (1999) Where is my arm? The relative role of vision and proprioception in the neuronal representation of limb position. Proc Natl Acad Sci USA 96:10418–10421
Graziano MS, Hu XT, Gross CG (1997) Visuospatial properties of ventral premotor cortex. J Neurophysiol 77:2268–2292
He SQ, Dum RP, Strick PL (1993) Topographic organization of corticospinal projections from the frontal lobe: motor areas on the lateral surface of the hemisphere. J Neurosci 13:952–980
He SQ, Dum RP, Strick PL (1995) Topographic organization of corticospinal projections from the frontal lobe: motor areas on the medial surface of the hemisphere. J Neurosci 15:3284–3306
Hepp-Reymond MC, Husler EJ, Maier MA, Ql HX (1994) Force-related neuronal activity in two regions of the primate ventral premotor cortex. Can J Physiol Pharmacol 72:571–579
Hepp-Reymond M, Kirkpatrick-Tanner M, Gabernet L, Qi HX, Weber B (1999) Context-dependent force coding in motor and premotor cortical areas. Exp Brain Res 128:123–133
Hoshi E, Tanji J (2002) Contrasting neuronal activity in the dorsal and ventral premotor areas during preparation to reach. J Neurophysiol 87:1123–1128
Johnson PB, Ferraina S, Bianchi L, Caminiti R (1996) Cortical networks for visual reaching: physiological and anatomical organization of frontal and parietal lobe arm regions. Cereb Cortex 6:102–119
Johnson MT, Coltz JD, Hagen MC, Ebner TJ (1999) Visuomotor processing as reflected in the directional discharge of premotor and primary motor cortex neurons. J Neurophysiol 81:875–894
Kakei S, Hoffman DS, Strick PL (2001) Direction of action is represented in the ventral premotor cortex. Nat Neurosci 4:1020–1025
Kalaska JF, Cohen DA, Hyde ML, Prud'homme M (1989) A comparison of movement direction-related versus load direction-related activity in primate motor cortex, using a two-dimensional reaching task. J Neurosci 9:2080–2102
Kawato M (1999) Internal models for motor control and trajectory planning. Curr Opin Neurobiol 9:718–727
Kurata K, Wise SP (1988) Premotor cortex of rhesus monkeys: set-related activity during two conditional motor tasks. Exp Brain Res 69:327–343
Li CS, Padoa-Schioppa C, Bizzi E (2001) Neuronal correlates of motor performance and motor learning in the primary motor cortex of monkeys adapting to an external force field. Neuron 30:593–607
Luppino G, Matelli M, Camarda R, Rizzolatti G (1993) Corticocortical connections of area F3 (SMA-proper) and area F6 (pre-SMA) in the macaque monkey. J Comp Neurol 338:114–140
Luppino G, Matelli M, Camarda R, Rizzolatti G (1994) Corticospinal projections from mesial frontal and cingulate areas in the monkey. Neuroreport 5:2545–2548
Matelli M, Luppino G, Rizzolatti G (1985) Patterns of cytochrome oxidase activity in the frontal agranular cortex of the macaque monkey. Behav Brain Res 18:125–136
Matelli M, Luppino G, Rizzolatti G (1991) Architecture of superior and mesial area 6 and the adjacent cingulate cortex in the macaque monkey. J Comp Neurol 311:445–462
Mauritz KH, Wise SP (1986) Premotor cortex of the rhesus monkey: neuronal activity in anticipation of predictable environmental events. Exp Brain Res 61:229–244
Mussa-Ivaldi FA, Bizzi E (2000) Motor learning through the combination of primitives. Philos Trans R Soc Lond B Biol Sci 355:1755–1769
Padoa-Schioppa C, Li CS, Bizzi E (2002) Neuronal correlates of kinematics-to-dynamics transformation in the supplementary motor area. Neuron 36:751–765
Padoa-Schioppa C, Li CS, Bizzi E (2004) Neuronal activity in the supplementary motor area of monkeys adapting to a new dynamic environment. J Neurophysiol 91:449–473
Riehle A, Requin J (1989) Monkey primary motor and premotor cortex: single-cell activity related to prior information about direction and extent of an intended movement. J Neurophysiol 61:534–549
Rouiller EM, Moret V, Tanne J, Boussaoud D (1996) Evidence for direct connections between the hand region of the supplementary motor area and cervical motoneurons in the macaque monkey. Eur J Neurosci 8:1055–1059
Saltzman E (1979) Levels of sensorimotor representation. J Math Psychol 20:91–163
Scott SH, Kalaska JF (1997) Reaching movements with similar hand paths but different arm orientations. I. Activity of individual cells in motor cortex. J Neurophysiol 77:826–852
Scott SH, Sergio LE, Kalaska JF (1997) Reaching movements with similar hand paths but different arm orientations. II. Activity of individual cells in dorsal premotor cortex and parietal area 5. J Neurophysiol 78:2413–2426
Shadmehr R, Moussavi ZM (2000) Spatial generalization from learning dynamics of reaching movements. J Neurosci 20:7807–7815
Shadmehr R, Mussa-Ivaldi FA (1994) Adaptive representation of dynamics during learning of a motor task. J Neurosci 14:3208–3224
Shen L, Alexander GE (1997a) Neural correlates of a spatial sensory-to-motor transformation in primary motor cortex. J Neurophysiol 77:1171–1194
Shen L, Alexander GE (1997b) Preferential representation of instructed target location versus limb trajectory in dorsal premotor area. J Neurophysiol 77:1195–1212
Thach WT (1978) Correlation of neural discharge with pattern and force of muscular activity, joint position, and direction of intended next movement in motor cortex and cerebellum. J Neurophysiol 41:654–676
Thoroughman KA, Shadmehr R (1999) Electromyographic correlates of learning an internal model of reaching movements. J Neurosci 19:8573–8588
Werner W, Bauswein E, Fromm C (1991) Static firing rates of premotor and primary motor cortical neurons associated with torque and joint position. Exp Brain Res 86:293–302
Wise SP, Mauritz KH (1985) Set-related neuronal activity in the premotor cortex of rhesus monkeys: effects of changes in motor set. Proc R Soc Lond B Biol Sci 223:331–354
Wolpert DM, Ghahramani Z (2000) Computational principles of movement neuroscience. Nat Neurosci 3(Suppl):1212–1217